M.A.L. Nicolelis (Ed.)
Progress in Brain Research, Vol. 130
© 2001 Elsevier Science B.V. All rights reserved

CHAPTER 10

Comparative population analysis of cortical representations in parametric spaces of visual field and skin: a unifying role for nonlinear interactions as a basis for active information processing across modalities

Hubert R. Dinse * and Dirk Jancke [1]

Institute for Neuroinformatics, Theoretical Biology, Ruhr-University Bochum, Bochum, Germany

Introductory

From a phenomenological point of view, the concept of population analysis is a rather straightforward and inescapable consequence of the observation that a huge number of broadly tuned neurons is activated after even the simplest form of sensory stimulation or in relation to motor outputs. This mass activity includes both spiking and suprathreshold activity. Our approach outlined in this chapter was developed in order to account for population activity recorded in early sensory cortices at a spiking level. Our goal was to visualize and to analyze cortical activity distributions in the coordinates of the respective stimulus space to explore cooperative processes (Dinse et al., 1996; Jancke et al., 1996; Kalt et al., 1996; Erlhagen et al., 1999; Jancke et al., 1999). The basic assumption is that neuronal interactions are an intricate part of cortical information processing generating internal representations of the environment beyond simple one-to-one mappings of the input parameter space. Using this approach, we can demonstrate that the spatio-temporal processing of sensory stimuli is characterized by a delicate, mutual interplay between stimulus-dependent and interaction-based strategies contributing to the formation of widespread cortical activation patterns.

Why populations?

In 1972, Barlow published the well-recognized article 'Single units and sensation: a neuron doctrine for perceptual psychology'. He proposed that "active high-level neurons directly and simply cause the elements of our perception" (Barlow, 1972). This work articulated the prevailing conceptual framework of that time and had a great impact on research of sensory information processing in early cortical areas. In fact, during the late fifties and sixties, single-cell recordings, the monitoring of extracellular potential changes, had become feasible routine in every laboratory. It is tempting to speculate, in how far purely technical aspects of that type boosted the conceptual framework of single-cell analysis.

While this approach became dominant during the next decades, at the same time, it became more and more evident that there might be more

* Corresponding author: Hubert R. Dinse, Institute for Neuroinformatics, Theoretical Biology, Ruhr-University Bochum, Bochum, Germany. Tel.: +49-234-32-25565; Fax: +49-234-32-14209;
E-mail: hubert@neuroinformatik.ruhr-uni-bochum.de
[1] Present address: The Weizmann Institute of Science, Rehovot, Israel.

to higher brain processes than revealed by single-cell recordings. It should be stressed that the emphasis on distributed population activity, instead of a single cell, does not imply the underestimation of the performance of single cells. On the contrary, there is more and more experimental evidence that axons, passive and excitable dendrites and spines play a possibly underestimated role in signal transfer and processing (Segev and Rall, 1998).

Anatomical analysis of cortical networks revealed the enormous richness of connectivity and interconnectedness of cortical networks (for review see Braitenberg and Schüz, 1991). According to their minute analysis, a single cortical cell receives on average synaptic inputs in the magnitude of 10^5. However, the proportion of direct sensory afferents is only 20% even in layer 4 that provides most of the sensory inputs. The degree of interconnectedness is best illustrated by calculations made by Braitenberg and Schüz (1991), according to which 1 mm^3 cortical volume contains about 150,000 neurons, 3 km axonal fibers and 450 m dendritic branches. Consequently, cortical networks are characterized by densely coupled widespread arborization of dendritic and axonal connections.

From a theoretical point of view, these anatomical constraints have been interpreted as an ideal substrate for parallel processing based on recurrent loops, in which lateral interactions and nonlinearities play a key role.

From a functional point of view, there is abundant evidence that is fully in line with the outlined theoretical and anatomical considerations:

(1) Cortical point-spread functions are broad. It is well established that widespread patterns of cortical activation are evoked by even very small and simple, i.e. 'point-like', stimuli. This is true for visual, auditory and somatosensory cortical areas. It simply implies that whatever the stimulus is, large populations of many thousands of neurons are invoked. It is interesting to note that most recent developed techniques to record neural activity do in fact measure equivalents of the cortical point spread function, as is the case for PET, fMRI and optical imaging of intrinsic or dye-coupled signals.

(2) Cortical processing is active. Neurons in striate visual cortex have been characterized with respect to physical key features, such as visual field location, orientation, motion direction, ocular dominance, and spatial frequency. These approaches allowed to analyze neural representations within parameter spaces that are explicitly defined by physical stimulus attributes. However, dependent on stimulus context, a large number of visual illusions, e.g. the perception of illusory contours (Kanizsa, 1976; Von der Heydt et al., 1984; Ramachandran et al., 1994; Sheth et al., 1996; Mendola et al., 1999), indicate that the visual system must contain additional mechanisms leading to representations within parameter spaces which have no physical counterpart. This is in line with the observation that single neurons exhibit complex, non-predictive behavior dependent on stimulus context (for review see Gilbert et al., 2000). Accordingly, this complex spatio-temporal response properties can be modified by stimulation displaced from the receptive field-center or even from outside the classical receptive field (Allman et al., 1985; Dinse, 1986; Gilbert and Wiesel, 1990; Sillito et al., 1995).

This can be rewritten by stating that if interaction contributes significantly to neural activation in the visual cortex, then representations of the visual environment will differ from a simple feedforward remapping of visual space.

(3) Behavioral performance is superior to single-cell performance. Except for a few examples, the performance inferred from single-cell tuning characteristics is not sufficient to explain the performance seen at a behavioral level. There are usually two responses to that: (a) neurons at higher (possibly unknown) stages of processing will show the required characteristics; and (b) the required performance will be generated as soon as a 'pool' of neurons is taken into consideration. A famous example is 'hyperacuity', the threshold of which is several fold beyond that of single cells (Westheimer, 1979). The 'coarse coding' framework is an attempt to explain how high resolution can be easily obtained with broadly tuned elements (Hinton et al., 1986).

Taken together, in order to address the implications listed above, the conceptual consideration of neural populations, their recording, analysis and understanding appears straightforward. A less straightforward question is how to accomplish this goal.

Emergence of de-novo representations?

As each single neuron is part of a population, a single neuron's activity is based on the entire network activity and vice versa, the network activity is dependent on the contributing single neurons. It has in fact been shown that the activity of a single neuron reflects the actual state of the entire neural network (Arieli et al., 1996; Tsodyks et al., 1999). Yet, an important question remains whether a population is able to create de novo 'qualia' neither explicitly present at the single-cell level nor in the input (Lehky and Sejnowski, 1999). The most prominent example might be the sensation of 'white' arising from the trichromatic color vision system (Young, 1802) by the joint activation of a population of retinal receptors tuned to different wavelengths. There are a number of recent experimental findings suggesting the population-based creation of de novo properties (Diesmann et al., 1999; Jancke, 2000; Thier et al., 2000).

Why parametric

In principle, when investigating the visual system, a distribution of population activity within the parametric space of the visual field is equivalent to activities recorded in functional imaging studies such as fMRI or optical imaging assuming a clean retinotopy. There are a number of differences, however. The main problem arises from the fact that the retinotopy is far from coming close to a clean representation of the visual field. This is particularly obvious at a spatial scale that differentiates between visual angles less than 1° apart (Hubel and Wiesel, 1962; Albus, 1975). The main constrains arise from the considerable scatter of RF position that is larger or in the same range than the required systematic shifts due to a topographic gradient in the map. Again, this holds true for other modalities in an analogous way.

At a larger scale of several degrees, a clear retinotopic gradient is present, though distorted. Yet at this scale, other factors complicate the aspect of a clean topography. As extensively studied in the visual system, the retinotopic gradient of the cortical map of the visual field is overlaid by so-called 'functional maps'. Functional maps contain an orderly arrangement of certain stimulus attributes in a repeated way for certain portions of the respective retinal locations (Hubener et al., 1997; Kim et al., 1999; Swindale, 2000). At present, functional maps have been established for orientation of moving gratings (Blasdel and Salama, 1986; Swindale et al., 1987; Bonhoeffer and Grinvald, 1991), direction of motion (Weliky et al., 1996) and the spatial frequency of the moving grating (Shoham et al., 1997; Kim et al., 1999). In addition, maps exist for the inputs of the two eyes (ocular dominance maps, Wiesel et al., 1974; LeVay et al., 1978) and disparity (Burkitt et al., 1998). There is, in fact, evidence that the retinotopic map contains discontinuities to account for the discrete organization according to certain stimulus attributes (Das and Gilbert, 1997). Taken together, the requirement for 'cleanness' of the map is not fulfilled at either spatial scale. For a discussion of multiple functional maps in auditory cortex, see (Schreiner, 1995).

Taken together, our parametric population approach takes into account that: (1) neurons are broadly tuned, e.g. covering large ranges of parameter values; and it enables (2) to analyze their common responses within the metrics of given stimulus attributes. In addition, the construction of distributions of population activity that are defined in physical metrics can help to find underlying neural transformation strategies that map sensory stimulus parameters onto the cortical anatomy.

Which metrics?

One fundamental question arises when discussing the metrics within which population of neurons should be studied. Probably the main advantage of the conventional single-cell receptive field (RF) approach was to describe neural activity within the metrics of the stimulus space, and not in the metrics of the anatomical connections, e.g. the dendritic branching of the cell. This simple remapping of activity made it possible to study the cell's firing as a function of any possible stimulus attribute in terms of its parameter space.

As detailed below, our approach similarly consists of a systematic remapping of population activity from their cortical coordinates back into the parametric space (Fig. 1). Accordingly, constructing

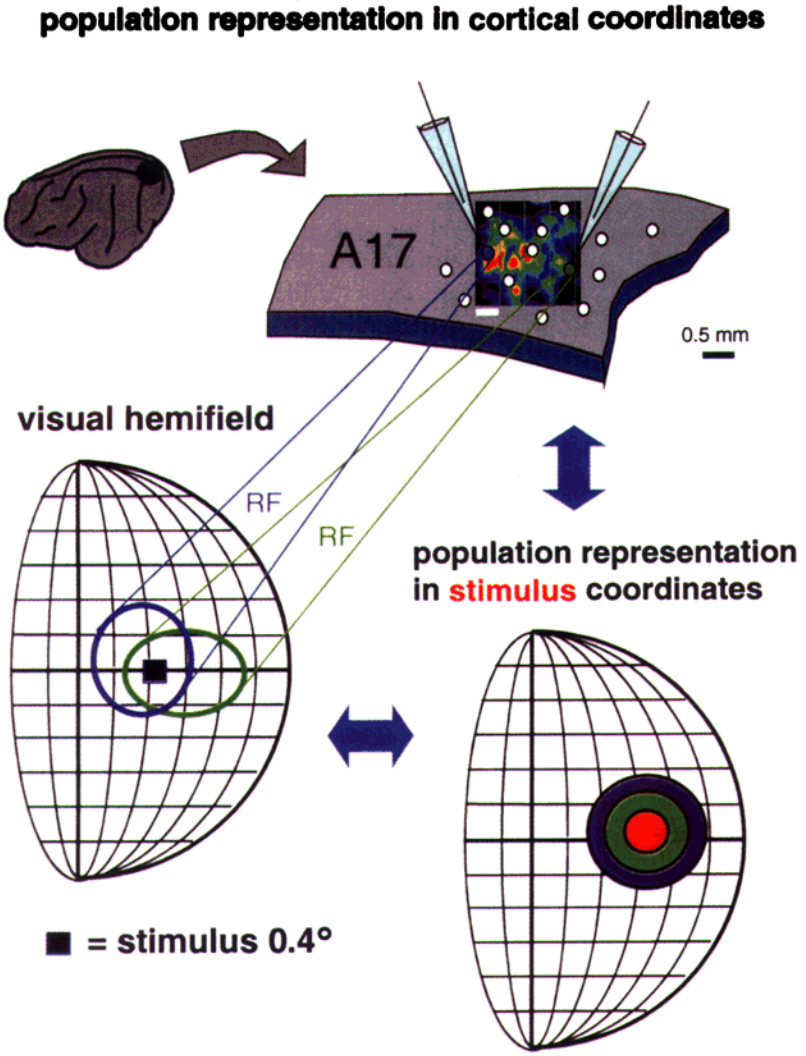


Fig. 1. Population representation in different coordinates exemplified for visual cortex studies. A stimulus is presented at a fixed location in the visual field (bottom, left). Recording of evoked activity results in a cortical activation corresponding to the cortical point spread function (top, right). Shown is an intrinsic optical imaging map evoked by a small square of light. Extracellular recordings of single cell responses (top, right) were used to determine the receptive fields (RFs) defined in the visual field coordinates (bottom, left, colored RF outlines). In contrast to conventional methodologies, we pursue a non-centered approach, in which a stimulus is kept at a fixed position independent from the location of the RFs being studied (bottom, left: relation of black square to RF outlines in blue and green, see also Fig. 2). The definition of single cell activity in parameter space allows a systematic investigation of the cells activity as a function of variation of stimulus parameter. Our approach accomplishes a transformation of population activity in parameter space which corresponds to a 'population RF' (see also Fig. 2). It should be noted that recording of activity across the cortical surface as obtained by optical imaging equivalently refers to a non-centered field approach. In contrast, a distribution of population activity in parameter space can be regarded as the inverted cortical point-spread function ('cortical spread-point function'. As a consequence, this procedure allows to investigate population distributions and their interactions in the physical metrics of the stimuli.

a parametric distribution of population activation can be regarded as a 'population receptive field'. We will demonstrate that this approach is highly suitable to reveal insight into processing principles, including neural interactions that go beyond those defined at the level of classical single-cell approaches.

Two types of averaging

Implication of the non-centered field approach

Our population approach is based on two different types of averages. Here we discuss the averaging across different spatial locations within the RFs.

In the conventional RF approach, stimuli are applied to the RF center. Accordingly, as a first step, the approximate shape and center of an RF has to be determined. Once that is done, stimuli of various types are presented at the center or along a centered orientation in order to study possible dependencies of the firing rate from stimulus variations. We call this procedure 'RF centered approach'. In contrast, as our main goal is to study a population response to a given stimulus, i.e. the contributions of all neurons responding in any way to a given stimulus, we keep the position of a stimulus fixed irrespective of the location and shape of the RF analyzed (Dinse and Jancke, 2001). This procedure is called the 'non-centered RF approach' (Figs. 1 and 2).

This procedure becomes intuitively clear when one considers how, under natural conditions, stimuli are distributed in relation to RFs. Only under extreme rare conditions will there be an RF-centered situation. Accordingly, outside the laboratory, visual objects are similarly distributed in arbitrary ways across RFs. In our view, this way of stimulus presentation and averaging is crucial for an understanding of how complex scenes are represented in the visual cortex. A similar approach has been pursued by van Essen and coworkers, who investigated the activity of visual cortex cells under natural viewing conditions (Gallant et al., 1998). In a way, this procedure corresponds to a systematic shift of a stimulus throughout an RF (cf. Szulborski and Palmer, 1990). Instead, we do not shift the stimulus, but sample the contributions of RFs of many neurons shifted randomly across the stimulus.

Multidimensional spaces, subpopulations, and the contributing neuron

A second important averaging is performed across many different cell types. Neurons in area 17 contribute potentially to the representations of many different parameters, such as retinal position, orientation, curvature, length, motion direction et cetera (see also above 'overlaying maps'). To characterize the contribution of each neuron to the representation of a given stimulus, one might conceive of the high-dimensional space spanned by its different parameters. Each neuron could be thought of as a point in this parametric space. This point corresponds to a set of preferred values for all represented parameters. By asking only how the neuron's firing rate depends on visual field position, the contributions of all neurons are averaged, although their preferred parameter set may be different along other dimensions. In this sense, the population distribution is a projection from a potentially high dimensional space onto a common neuronal space representing only visual field position (Jancke et al., 1999). In this way, the 'population receptive field' can be regarded as the inverse of the cortical point-spread function ('cortical spread-point function').

Reconstruction of information

There is agreement that physical attributes of sensory stimuli are encoded as activity levels in populations of neurons. Reconstruction or decoding describes the inverse problem in which the physical attributes are estimated from neural activity. Reconstruction methods have been regarded useful first in quantifying how much information about the physical attributes is present in a neural population and, second, in providing insight into how the brain might use distributed activity (Nicolelis, 1996; Zhang and Sejnowski, 1999; Doetsch, 2000). However, given that: (a) an optimal reconstruction method is utilized; (b) the population is of sufficient size, i.e. it contains a sufficient number of neurons; and (c) the stimuli are within the range of behavioral relevance and resolution, i.e. belong to a stimulus that is represented in the brain, we argue that the mere reconstruction does not yield much additional information.

Of course, one of the problems behind this is the question who reads the code. In the case of optimal reconstruction, an implicit assumption is that the brain is able to perform a comparable analysis. Ways to prove this assumption are to compare population data with psychophysical data of performance, thresholds, discrimination abilities, reaction times etcetera. An ultimate control consists of execution of behavior,

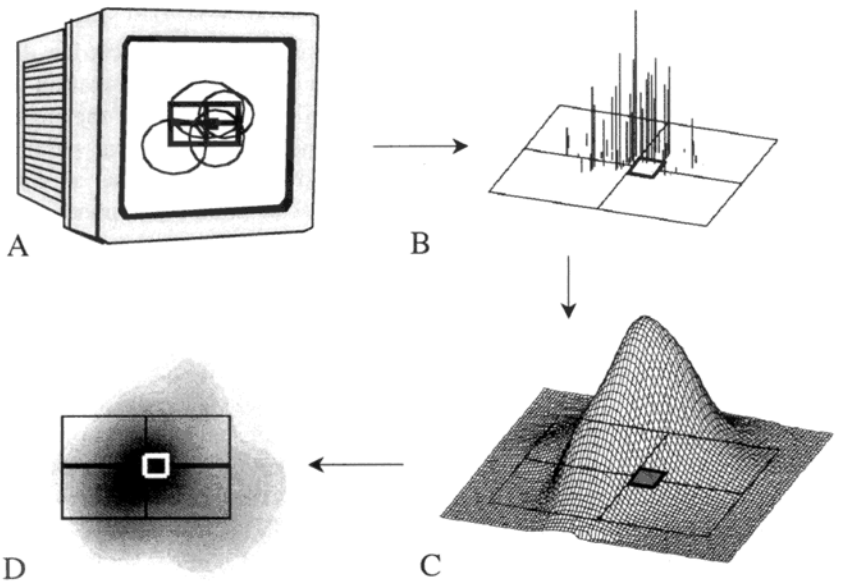


Fig. 2. Schematic illustration of stimulation and construction of population distributions exemplified for the visual cortex. (A) Illustration of the non-centered field approach. Stimuli, indicated by the black square, were presented independent of the locations of the receptive fields (RFs) of the measured neurons (schematically illustrated by the ellipses). The frame with the cross-hair (gray) illustrates the analyzed portion of the visual space (2.8 × 2.0). (B–D) Illustrations of the Gaussian interpolation method to construct the distribution of population activity. (B) The location of the RF center of each neuron as determined by response plane techniques was weighted with its firing rate, illustrated as vertical bars of varying length at various locations. (C) The distribution of population activity was obtained by Gaussian interpolation (width = 0.6°). (D) View of the distribution of population activation using gray-levels to indicate activation. The location of the stimulus is indicated by the square outlined in white together with the stimulus frame. In the results section, activity distributions are shown as color-coded contour plots.

as exemplified in the study by Chapin et al. (1999), where rats were trained to position a robot arm to obtain water by pressing a lever. Mathematical transformations were used to convert multineuron signals into 'neuronal population functions' that accurately predicted lever trajectory and were used by the animals as a substitute of executed behavior to position the robot arm and obtain water. More generally, during recent years, it became evident that a critical step for the investigation of how distributed cell assemblies process behaviorally relevant information is the introduction of methods for data analysis that could identify functional neuronal interactions within high dimensional data sets (cf. Nicolelis, 1999).

What is gained: neural interaction information

Our approach seeks an alternative in comparing different states of population activity evoked by different classes of stimuli. Instead of asking how accurately the parameter of for example stimulus location can be reconstructed or decoded, we primarily were interested in analyzing interaction-based deviations of population representations dependent on defined variations of stimulus configurations. Accordingly, there is an important point of departure from the interest we share with aspects relating to estimation theory. Instead, our analysis aimed to investigate how the representation of position is affected by interaction among neurons.

The impact of interaction on human perception has been repeatedly shown. Repulsion effects between neighboring stimuli have been described in humans. Errors incurring when subjects estimate the visual distance between two spots of light depend systematically on the retinal distance of the stimuli. Small separations are underestimated, large distances are overestimated (Hock and Eastman, 1995). Similar results have been obtained for estimation of the orientation of stimuli (Westheimer, 1990).

In the experiments described below, we introduce similar paradigms contrasting population activ-

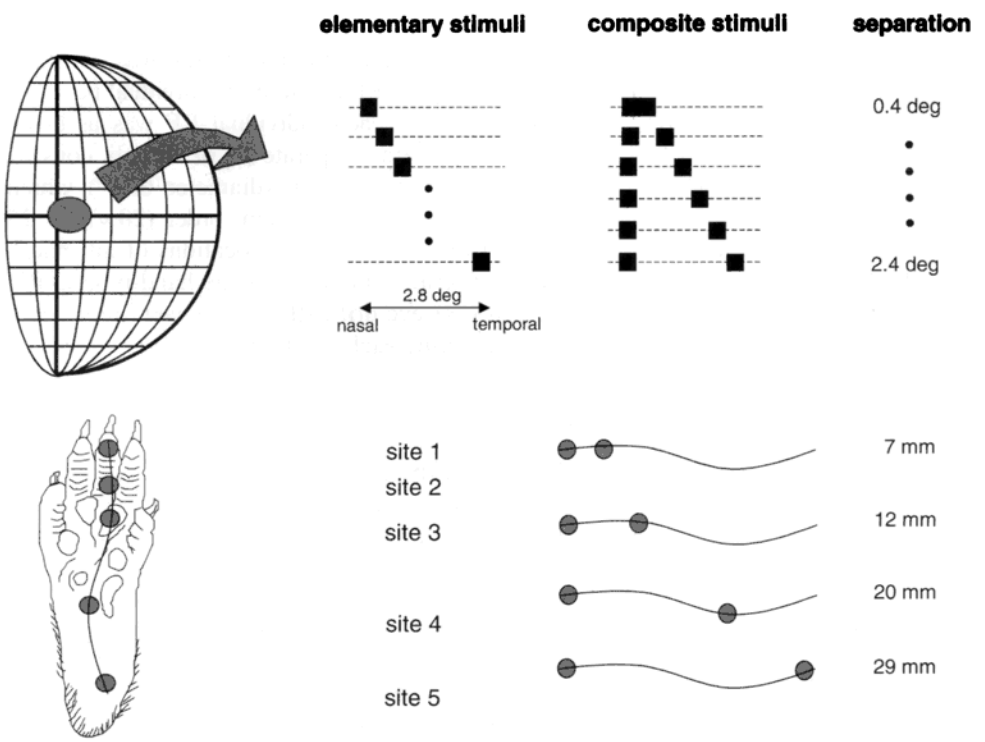


Fig. 3. Comparison of stimulation configurations used for the investigation of nonlinear interaction in the visual and the somatosensory cortex. Stimuli employed were small squares of light (cat visual cortex) and small tactile stimuli (light taps) applied to the glabrous skin of the hindpaw (rat somatosensory cortex), which were denoted as elementary stimuli. Top row: in the visual cortex, the elementary stimuli (squares of light, $0.4 \times 0.4°$) were presented at seven horizontally shifted positions within the central visual field representation. Bottom row: in the somatosensory cortex, elementary stimuli (1.5 mm in diameter) were presented at five positions along the distal–proximal axis of the hindpaw. Both studies had in common that composite stimuli were assembled from combinations of the elementary stimuli. In the visual cortex, they were presented at six different separation distances of 0.4–2.4° (top row). The left stimulus component was always kept at a fixed nasal position. In the somatosensory cortex, the composite stimuli were presented at four different separation distances between 7 and 29 mm skin surface (bottom row). The most distal stimulus component (site 1) was always kept fixed.

ity resulting from so-called 'simple' or 'elementary' stimuli with composite stimuli that were assembled from the elementary ones using different separation distances (Fig. 3). In detail, we extract the contribution of neurons to the representation of the location of small squares of light which we called 'elementary' stimuli. We then project the neural responses to 'composite' stimuli assembled from the two elementary stimuli of varied separations onto this subspace by analyzing population distributions weighted with the responses to composite stimuli.

If nonlinear interactions contribute significantly to neural activation in the visual cortex, then the representations of composite stimuli will systematically differ from the superposition of two elementary. Insight into neural interactions of the analysis of distance-dependent deviations of the distributions from additivity, i.e. how interactions distort the distributions of activation. Such interactions may arise from recurrent connectivity within the cortical area as well as from recurrency within the network providing the sensory input.

Methodological considerations and population construction

Construction of a distribution of population activation

Our general idea behind constructing a population distribution is to extract the contributions of neurons to the representation of a particular stimulus param-

eter. To obtain entire distributions that are defined for sensory field location, two types of analysis were applied (for details see Appendix):

(1) Based on the measured RF profiles, the calculated RF centers served to construct two-dimensional distributions of population activity by interpolating the normalized firing rates of each contributing neuron with a Gaussian profile. Calculation of population representations in the somatosensory cortex based on an analogous Gaussian interpolation

(2) To minimize the reconstruction error for the elementary stimulus conditions, we extended the Optimal Linear Estimator (OLE) (Salinas and Abbott, 1994) resulting in one-dimensional distributions of population activity.

Data acquisition: visual cortex

We recorded responses of single units in the central visual field representation in area 17 of the left hemisphere of anesthetized cats. Stimuli were always presented to the contralateral eye. Recordings were performed simultaneously with two or three glass-coated platinum electrodes (resistance between 3.5 and 4.5 MOhm, Thomas-Recording, Germany). The bandpass-filtered (500–3000 Hz) electrode signals were fed into spike sorters based on an on-line principle component analysis (Gawne and Richmond, NIH, USA).

Visual stimulation

Stimuli were displayed on a PC-controlled 21-inch monitor (120 Hz, non-interlaced) positioned at a distance of 114 cm from the animal.

An identical set of common stimuli was presented to all neurons: (1) elementary stimuli (Fig. 3), small squares of light (size 0.4 × 0.4°), were flashed at one of seven different horizontally contiguous locations within a fixed reference frame; and (2) composite stimuli, two simultaneously flashed squares of light, were separated by distances that varied between 0.4 and 2.4°. Each stimulus was flashed for 25 ms. The interstimulus interval (ISI) was 1500 ms. There was a total of 32 repetitions of each stimulus, arranged in pseudo-random order across the different conditions. Stimuli had a luminance of 0.9 cd/m^2 against a background luminance of 0.002 cd/m^2. The retinal position of these common stimuli was constant, irrespective of the RF location of individual neurons.

The profile of each individual RF was assessed quantitatively with a separate set of stimuli, consisting of small dots of light (diameter 0.64°) which were flashed in pseudo-random order (20×) for 25 ms (ISI 1000 ms) on the 36 locations of an imaginary 6 × 6 grid, centered over the hand-plotted RF. To control for eye drift, RF profiles were repeatedly measured during each recording session.

Data acquisition: somatosensory cortex

Single unit activity was extracellularly recorded in layer III–IV of the primary somatosensory cortex of anesthetized rats at depths of 700–750 μm using glass micro-electrodes filled with concentrated NaCl (1–2 MOhm). The bandpass-filtered (500–3000 Hz) electrode signals were fed into a window discriminator. The output TTL-pulses were stored on a PC with a time resolution of 1 ms. Raw analog recordings were displayed on oscilloscopes and on audio monitors. Digitized neural responses were displayed as post-stimulus time-histograms (PSTHs) on-line during the recording sessions. Data were analyzed off-line in the IDL graphical environment (RSI, USA).

Tactile stimulation

Penetrations were usually placed 200–300 μm apart to map the entire spatial extent of the hindpaw representation. The location and extent of RFs on the glabrous skin of the hindpaw was determined by hand-plotting (Merzenich et al., 1984). RFs were defined as those areas of skin at which just visible skin indentation evoked a reliable neural discharge. Other studies have shown that just-visible indentation is in the range of 250–500 μm, which is in the middle of the dynamic range of cutaneous mechanoreceptors (Johnson, 1974; Gardner and Palmer, 1989). Cells responding either to high threshold stimuli, joint movements or deep inputs were classified as non-cutaneous and were excluded from further evaluation. The size (area of skin in mm^2) of cutaneous RFs was quantitatively analyzed by planimetry.

For the analysis of neural population representations, an identical set of computer-controlled so-

called 'common stimuli' was presented to all neurons recorded independent from their RF location (non-RF-centered approach). For this type of stimulation, five plungers with tip-diameters of 1.5 mm were used. The plungers were mounted on a movable arm so that the stimulators could be positioned with high accuracy at selected positions of the rat hindpaw. A computer interface was used to control timing and forces of stimulation. As describe for handplotting, the plungers were adjusted to evoke indentation in the range of 250–500 μm.

(1) Single elementary stimuli consisted of simple tappings. These stimuli were applied to five always identical positions on the rat hindpaw arranged along the distal–proximal extension from the tip of digit 3 to the palm, designated as site 1 to site 5 (Fig. 3).

(2) Composite stimuli consisting of two simultaneously applied taps assembled from the single elementary stimuli, separated by distances varying between 7 and 29 mm (combining stimulation of sites 1-2, 1-3, 1-4 and 1-5). The duration of each tap was 8 ms. The stimuli were presented in a pseudo-random order at 32 repetitions with an ISI of 1000 ms.

Towards an understanding of neural interactions: application of the population coding approach in two different modalities

Here we summarize recent findings, in which we explore the role of neural interactions for the representation of sensory stimuli in early cortical areas. In detail, we describe the distance-dependent interactions for composite stimuli observed in the visual and the somatosensory cortex that share substantial similarities.

Distance-dependent interactions for composite stimuli observed in cat visual cortex

We constructed distributions of population activity in response to a set of small squares of light (so-called 'elementary stimuli') which differed in their position along a virtual horizontal line (Figs. 3 and 4).

The distributions were defined in the visual space and were based on single-cell responses from 178 neurons recorded in the central visual field representation of cat area 17. In order to obtain these distributions, we used a two-dimensional Gaussian interpolation procedure, in which the RF centers were weighted with the normalized firing rate of each neuron. Neural responses obtained during the entire time course of responses were analyzed (30–80 ms after stimulus onset). The width of the Gaussian was chosen uniformly to 0.6° to match the experimentally derived average RF profile of all neurons (cf. Jancke et al., 1999). In addition, based on the assumption that the representation of visual location can be considered as a function of activation in parameter space, we minimized the error for reconstructing one-dimensional distributions using the optimal linear estimator (OLE) procedure. This method is optimal in the sense that it extracts the available information from the firing rates under the condition of a least square fit. Both approaches yielded equivalent results. For the OLE-derived results and for a time-resolved approach that captured the dynamics of neuron responses and the analysis of interaction dynamics see Jancke et al. (1999).

As illustrated in Fig. 4, the interpolation derived activity distributions were monomodal and centered onto each respective visual field position (indicated by white squares). The spatial arrangement of activity of these distributions implies that neurons in primary visual cortex contribute as an ensemble to the representation of visual field location although each neuron's RF might be broadly tuned to stimulus location, i.e. is characterized by RF sizes several fold larger than the stimuli employed.

As discussed above, the mere construction of these representations does not provide much information about ongoing processing mechanisms. We therefore asked the question in how far the representation of composite stimuli consisting of two elementary stimuli can be predicted from the representations of the elementary ones, thereby addressing the question of neural interactions within the population representation. If there were no interactions within the population, then the distributions of the composite stimuli would be predicted to be the linear superpositions of the distributions of the component elementary stimuli. To test this hypothesis, we build distributions based on the same estimator used for elementary stimuli, but now weighting each cell's contribution with the firing rate observed in response to the composite stimuli. Fig. 5 illustrates the distributions of composite stimuli and their super-

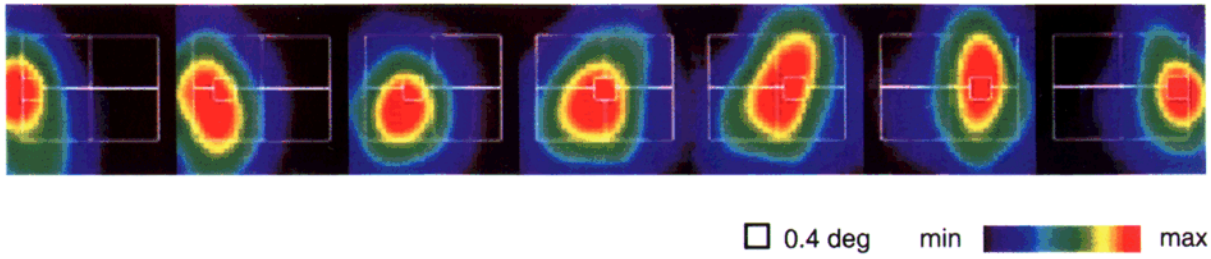


Fig. 4. Population representations of the seven elementary stimuli (cf. Fig. 3) recorded in cat visual cortex computed as two-dimensional activity distributions over visual space after Gaussian interpolation (cf. Figs. 1 and 2). The construction was based on spiking activity of 178 neurons. The distributions were computed in the time interval between 40 and 65 ms after stimulus onset corresponding to the neural peak responses. The activation level is shown in a color-scale normalized to maximal activation separately for each stimulus. Red indicates high levels of activation. The frame outlined in white depicts the region of the visual field that was investigated (cf. Fig. 3). In addition, the stimulus is shown as a square outlined in white. Note that for each stimulus, position the focal zone of activation is approximately centered on the stimulus. Reproduced, with premission, from Jancke et al., 1999. Copyright 1999 by the Society for Neuroscience.

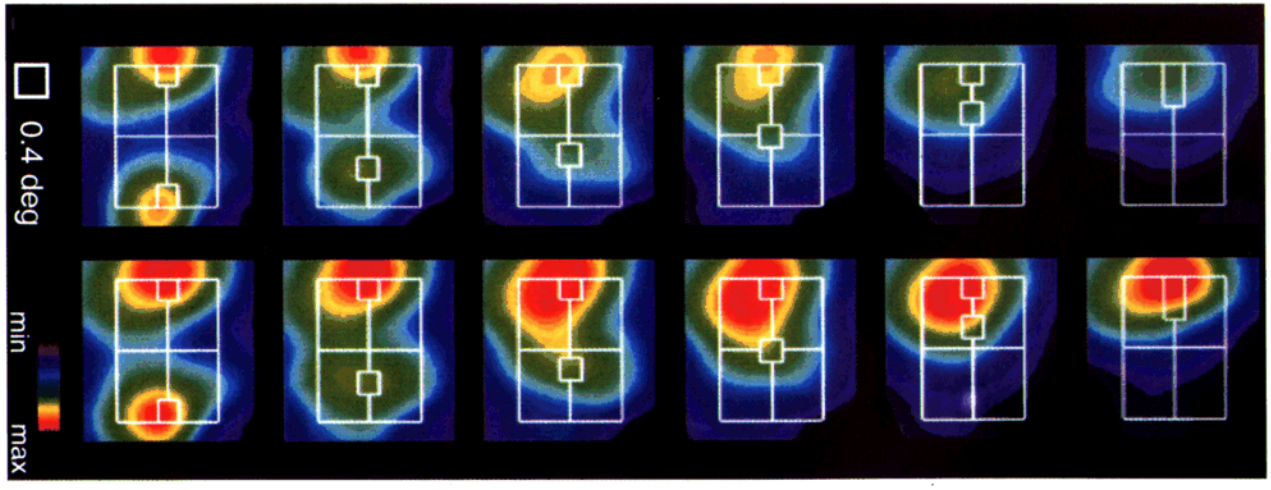


Fig. 5. The measured two-dimensional activity distributions recorded in the visual cortex of the six composite stimuli (left, from top to bottom: 0.4–2.4° separation, cf. Fig. 3) were compared to the superpositions of their component elementary stimuli (right). The activity distributions were based on spike activity of 178 cells averaged over the time interval from 30 to 80 ms after stimulus onset. Same conventions as in Fig. 4, the color-scale was normalized to peak activation separately for each row. For small stimulus separation, note the remarkably reduced level of activation for the measured as compared to the superimposed responses. This behavior could not be explained by saturation effects, see text). A transition from monomodal to bimodal distributions was found between 1.2 and 1.6° separation. The bimodal distribution recorded for the largest stimulus separation comes close to match the superposition. However, inhibitory interaction can still be observed. An asymmetry in the shape and amplitudes between the representations of the left and the right stimulus component was present for the measured as compared to the superimposed distributions, specifically for stimulus separations of 1.2 and 1.6°. Reproduced, with premission, from Jancke et al., 1999. Copyright 1999 by the Society for Neuroscience.

positions. Both, the measured and the superimposed distributions of population activity were monomodal for small, and bimodal for large stimulus separations, the transition occurring at around 1.6° separation.

The most striking deviation from the linear superposition was a reduction of activity compared to the measured responses, which was particularly strong for small stimulus separations. This reduction was not due to a saturation of population activity since it was also observed for composite stimuli of larger separations, where the distributions were bimodal and had little overlap (for a more extended discussion, see Jancke et al., 1999).

A quantitative assessment of this suppressive interaction allowed to uncover its dependence on stimulus distance. The total activation in the population distribution was computed as the area under the distribution and was expressed as a percentage of the total activation contained in the superposition. This percentage was always below 100%, confirming the inhibitory effect as a consequence of using composite stimuli. Suppression was strongest for small distances and decreased with increasing distances (Fig. 6).

To quantitatively assess the accuracy with which the distributions of population activity represent location, we compared the position of the maximum

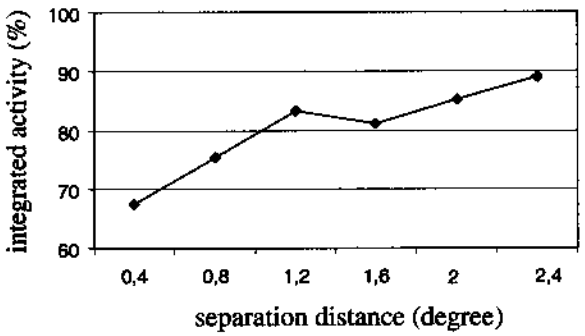


Fig. 6. Interaction based suppression of the population activity recorded in cat visual cortex induced by composite stimuli as a function of separation between the two component stimuli. The total activation in the distribution was expressed as a percentage of the total activation in the superposition. Inhibition was strongest for zero distance (0.4°separation) and decreased almost monotonically with increasing distance, but was still present at the largest separation tested (2.4°).

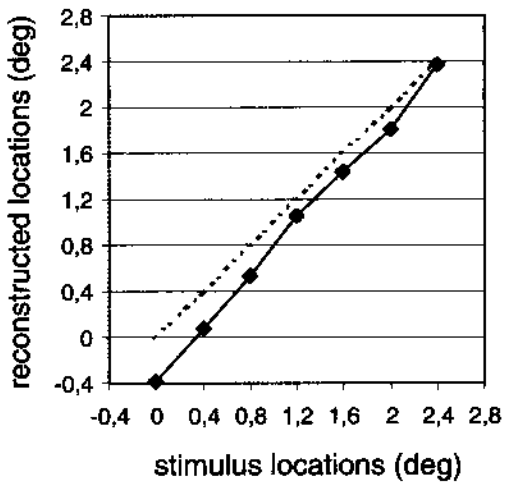


Fig. 7. Constructed versus real position of the elementary stimuli using the averaged spike activity. The positions of the maximum of the population distributions are shown for the seven elementary stimuli as a function of the real stimulus position. The dotted line indicates the perfect match between estimated and real stimulus position. Stimulus position can be accurately estimated; however, there is a systematic deviation in localization for all locations that might reflect a true mislocalization as described recently for human perception.

of each distribution to the respective stimulus position. Fig. 7 plots these constructed positions against the real stimulus positions. For all positions tested, there was a systematic deviation of on average $0.20\pm0.11°$. Interestingly, in a recent psychophysical

study, briefly presented stimuli have been found to be mislocalized. When observers were asked to localize the peripheral position of a probe with respect to the midposition of a spatially extended comparison stimulus, they tend to judge the probe as being more toward the periphery than is the midposition of the comparison stimulus (Müsseler et al., 1999). It might therefore be speculated that the systematic error is not due to a bias in sampling RFs or due to errors in reconstruction, but instead reflect a true mislocalization in the representation.

Distance-dependent interactions for composite stimuli observed in rat somatosensory cortex

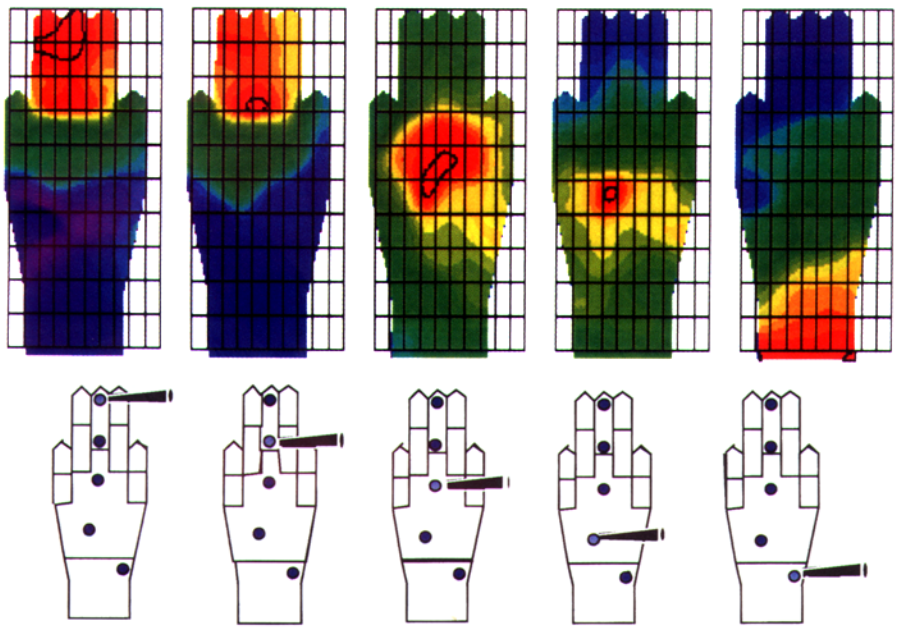
Similar to our procedure utilized for the exploration of interaction effects in cat visual cortex, we constructed distributions of population activation in response to a set of small tactile stimuli which differed in their position along the distal–proximal extension from the tip of digit 3 to the palm. In analogy to the visual cortex study, these stimuli were termed 'elementary stimuli'. The distributions of population activity were derived from single-cell responses from 206 neurons recorded in the hindpaw representation of rat somatosensory cortex. They were obtained after backprojection of cortical activity onto stimulus space and can be regarded as a population receptive field defined in skin space. Similar to the visual cortex study, we used a two-dimensional Gaussian interpolation procedure, in which the RF centers were weighted with the normalized firing rate of each neuron. As the distribution of all recorded RFs was not homogenous, a higher number of neurons were sampled at the distal part of the paw representation, the population activity was normalized for sampling density.

The resulting color coded activity distributions of the neural population are depicted in Fig. 8. The corresponding stimulus configuration is indicated in a schematic drawing. The areas with maximum population activity matched fairly well the sites of tactile stimulation, except for the representation of the proximal hindpaw of stimulus site 5, where we observed a fairly broad distribution without a sharp peak of activity. The shape of the distributions showed a substantial degree of variability, a finding not that evident for visual representations. The activity distributions for stimulation of sites 2 and 4 were rather distinct compared to the population representations for stimulation sites 1 and 3. The activity distribution was scaled to cover the whole color table in order to illustrate the shape of the population distributions. Quantitative assessment revealed that the population response amplitudes varied only by about 15% between sites 1 and 4. Despite the density normalization, activity at site 5 reached only 55% of the maximum activity elicited at site 4. We therefore assume that the weak population response of this site might reflect a genuine difference of the cortical representation of this very proximal part of the hindpaw.

Fig. 8. Population representations of the five elementary stimuli (cf. Fig. 3) recorded in rat somatosensory cortex depicted as two-dimensional activity distributions (top) over the glabrous skin surface of the hindpaw (cf. Figs. 1 and 2). The construction was based on the activity of 206 neurons. Activity distributions were computed in the time interval between 16 and 30 ms after stimulus onset corresponding to the neural peak responses. The activation level is shown in a color-scale normalized to maximal activation separately for each stimulus. The grid overlying the distribution is intended to facilitate localization of activity. Red indicates high levels of activation. Bottom: figurines of the hindpaw indicate schematically position of the elementary stimuli. Note that for each stimulus, the focal zone of activation is fairly centered on each stimulus location.

To address the question of neural interaction dynamics within the population representations, we compared the activity distribution obtained for composite stimuli to their superpositions. As in the visual cortex study, evidence for interactions was inferred from deviations of the population representations of the composite stimuli from the linear superpositions of the component elementary stimuli. We therefore build population representations based on the same estimator used for elementary stimuli, but now weighting each cell's contribution with the firing rate observed in response to the composite stimuli.

In Fig. 9, the population activity distribution for the measured and the superimposed distributions are illustrated. The measured distributions were monomodal for smaller stimulus separations (stimuli 1-2 and 1-3, 7 and 12 mm). Bimodal distributions were only found for larger separations of 20 and 29 mm (stimuli 1-4 and 1-5). Similar to what we had found in the visual cortex, the most striking devia-



tion from the linear superposition was a reduction of activity compared to the measured responses. Again, this suppressive effect was particularly strong for smaller stimulus separations between 7 and 12 mm. The distance-dependent suppression was quantified

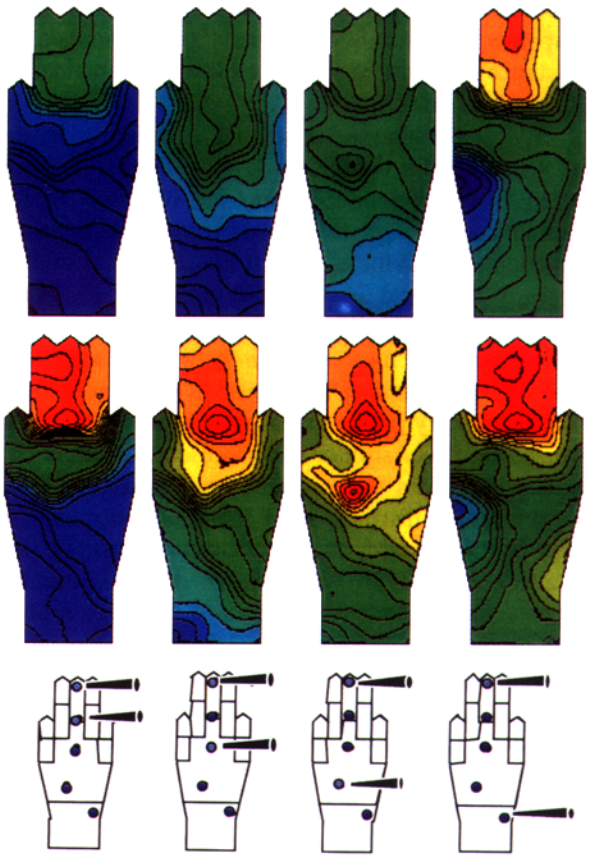


Fig. 9. The measured two-dimensional activity distributions recorded in rat somatosensory cortex of the four composite stimuli (top, from left to right: 5–24 mm skin surface separation, cf. Fig. 3) were compared to the superpositions of the representations of their component elementary stimuli (middle). The activity distributions were based on spike activity of 206 cells averaged over the time interval from 16 to 30 ms after stimulus onset. Same conventions as in Fig. 8, the color-scale was normalized to peak activation separately for each column. For small stimulus separation, note the remarkably reduced level of activation for the measured (top) as compared to the superimposed (middle) responses. The measured distributions were monomodal for smaller stimulus separations (stimuli 1-2 and 1-3, 7 mm and 12 mm). Bimodal distributions were only found for larger separations of 20 and 29 mm (stimuli 1-4 and 1-5). The bimodal distribution recorded for the largest stimulus separation comes close to match the superposition. As in the case of the visual cortex study, inhibitory interaction can still be observed. An asymmetry in the shape and amplitudes between the representations was present for the measured as compared to the superimposed distributions, with the tendency of an attraction of activity towards the distal aspects of the hindpaw.

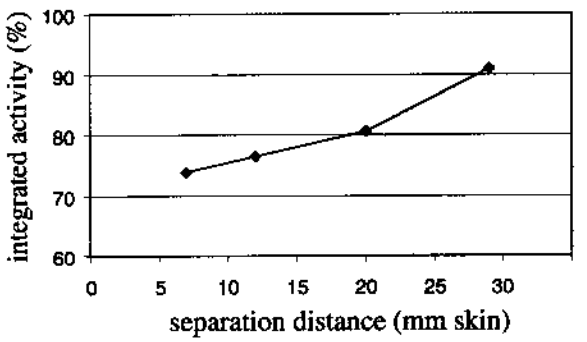


Fig. 10. Interaction based suppression of the population activity recorded in the somatosensory cortex induced by composite stimuli as a function of separation between the two component stimuli. Similar to our findings in the visual cortex (cf. Fig. 6), the total activation in the distribution was expressed as percentage of the total activation in the superposition. Inhibition was strongest for the smallest separation tested and decreased almost monotonically with increasing distance, but was still present at the largest separation tested (29 mm skin surface).

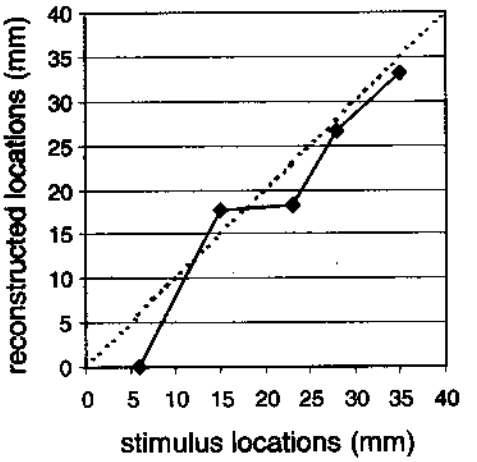


Fig. 11. Constructed versus real position of the elementary stimuli using the averaged spike activity. The positions of the maximum of the population distributions are shown for the five elementary stimuli as a function of the real stimulus position. The dotted line indicates the perfect match between estimated and real stimulus position. Stimulus position can be accurately estimated, however, fluctuations appear to be more random.

by expressing the integrated population activity in the measured distributions to those obtained from superposition. As shown in Fig. 10, we found a clear distance dependence very similar to that obtained in the visual cortex.

We also found a substantial asymmetry in the distributions for composite stimuli (Fig. 9) that was even more pronounced than that observed in the visual cortex. This asymmetry consisted in an attraction of activity evoked from composite stimuli towards the distal aspects of the hindpaw, i.e. in the direction of the digit representation. It is well known that the cortical map of the hindpaw is dominated by the representation of the digits. In contrast, a similar asymmetry in the visual field representations at the scale of our stimuli is not present. In single-cell recordings from monkey area 3b, a systematic bias in the spatial distribution of inhibitory surrounds of tactile RFs towards the fingertip was reported (DiCarlo et al., 1998). We therefore conclude that the substantial asymmetry found in SI probably reflects the representational constraints present in the somatotopic representation.

In order to illustrate the accuracy with which the population distributions represent locations within the skin of the hindpaw, the coordinates along the distal to proximal dimension of the locations with maximal activity levels were plotted as function of the real stimulus location. Points on the diagonal indicate an ideal representation of the stimulus location. The distance of the points from the diagonal is a measure for the discrepancy of the reconstructed with the real stimulus locations. As shown in Fig. 11, the reconstructed locations were usually shifted to the proximal portions of the paw. Only in the case of stimulation at site 4, the reconstructed stimulus location is situated more distally compared to the actual position. We are not aware of any psychophysical evidence for a systematic mislocalization towards the tip of the hands, although there are many reports of significant mislocalizations after plastic reorganizations (Sterr et al., 1998; Braun et al., 2000). Accordingly, it remains an open question as to how far the observed errors in localization reflect shortcomings in RF sampling.

Using a population of 206 neurons, the stimulus position could be reconstructed with an accuracy of ± 3.39 mm, given an average RF size of 56 mm^2 (cf. Fig. 11). Recently, it had been reported that simultaneous multi-site neural ensemble recordings in three areas of the primate somatosensory cortex (areas 3b, SII and 2) consisting of small neural ensembles (30–40 neurons) of broadly tuned somatosensory neurons were able to identify correctly the location of a sin-

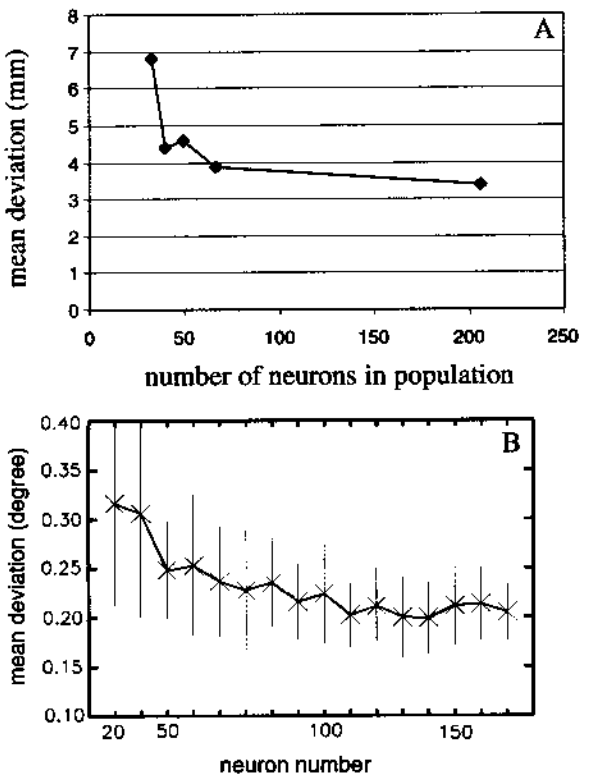


Fig. 12. (A) Average deviation of the activity distributions from an ideal localization of the stimulated sites as a function of neuron numbers in the somatosensory cortex. There is a fairly strong reduction in the deviation from ideal localization when the number of neurons is increased from 30 to 40 cells. Further increase of neuron number yields only little further increase in performance of localization. (B) Average deviation of the activity distributions from an ideal localization of the stimulated sites as a function of neuron numbers in the visual cortex. Similar to the data from somatosensory cortex, the most prominent gain in localization is obtained for a fairly small size of population in the range of 40–50 neurons.

gle tactile stimulus on a single trial (Nicolelis et al., 1998). We performed a type of bootstrap analysis, in which neurons from the entire population were randomly selected to generate subpopulations of 33, 40, 50 and 67 neurons. Re-analysis of the data showed that the localization error was significantly reduced when we increased the number of neurons from 33 to 40, while further increase yielded little further improvement in localization (Fig. 12A). Interestingly, a similar analysis performed in the visual cortex revealed a comparable dependency on neuron number (Fig. 12B).

Similarities and differences of population representation of simple elementary stimuli and resulting interactions from composite stimuli

Our goal was to explore the general relevance of active, cooperative processes in the representation of simple sensory stimuli by comparing neural interaction effects recorded in primary visual and somatosensory areas. We therefore constructed sets of stimuli that combined aspects of simplicity with aspects of comparability. In our view, small squares of light displayed in the visual field at contiguous locations along a virtual horizontal line might be maximal equivalent to small taps of cutaneous stimuli presented at adjacent locations along the distal–proximal axis of the glabrous skin of the paw. Most importantly, in both cases, the composite stimuli were assembled from these elementary stimuli to yield a set of 'complex' stimuli of variable separation distances (cf. Fig. 3). Under these assumptions, we could demonstrate considerable similarities of the overall properties of population activity recorded in the visual and the somatosensory cortex:

(1) Population activity in the parametric space of the visual field or the hindpaw glabrous skin could be characterized by sharply focused distributions centered around the location of the stimulus.
(2) The distributions evoked by the composite stimuli could not be predicted from the superpositions of the distributions obtained for the elementary ones.
(3) Accordingly, in both modalities, nonlinear interactions played an important role in the generation of 'complex' representations.
(4) The effects of interactions consisted of a substantial suppression of response that was dependent on separation distance between the stimuli.
(5) The amount of inhibition seen and the slope of the distance–response function were similar, indicating that the metrics that govern the interactions are comparable, despite their enormous differences in physical attributes.
(6) Analyzing the number of neurons necessary to yield a given performance resulted in a comparable population size.

However, we also observed a number of dissimilarities. The observed differences mostly deal with aspects of asymmetry within the representation.

Most notably, while population activity in the parametric space of the visual field was fairly similar in amplitude and shape across the seven elementary stimuli, we observed a gradient in amplitude in the representations of the tactile stimuli, with the representation of the most proximal aspects of the hindpaw being considerable weaker and broader.

Embedding parametric maps and interaction ranges in cortical anatomy

It remains to be clarified in how far the similarities of distance-dependence of interactions translate into the metrics of their respective cortical representations. In order to provide a first approximation, we take into account the mapping experiments of Tusa and coworkers in cat visual cortex (Tusa et al., 1978). According to their data, 2.8° of the central visual field corresponds roughly to an area of 3 mm cortical surface. In contrast, the dimensions of the rat hindpaw map in primary somatosensory cortex is in the range of 1–1.5 mm (Chapin and Lin, 1984). This comparison implies that comparable interaction mechanisms might operate on spatial scales of cortical coordinates that differ by a factor of two. It has been speculated that long-range horizontal connections are instrumental in providing a substrate mediating the interaction effects. Wide-spread horizontal connections have been described for visual cortex spanning several millimeters (Gilbert and Wiesel, 1985; Löwel and Singer, 1992; Kisvarday et al., 1997; Sur et al., 1999). In addition, short range interactions have been shown to be involved in contextual modulations (Das and Gilbert, 1999). It is conceivable that the spatial ranges of short- and long-range connections are different in rat cortex (cf. Hickmott and Merzenich, 1998; Cauller et al., 1998), thereby providing a species- and modality-specific adaptational scaling to the needs of interaction dimensions (Dinse and Schreiner, 2001).

Conclusions

We used a population coding approach to visualize and to investigate representations of simple sensory stimuli in terms of their parametric spaces. We provided evidence that nonlinear interactions are crucially involved in the generation of representations evoked by composite stimuli built from simple ones. This approach was applied in studies of the visual and somatosensory cortex to address the question about a possible modality and area-independent role of neural interactions (Dinse and Schreiner, 2001).

We found that the population activity to elementary and composite stimuli shared a number of substantial similarities. Most notably, we found a comparable distance-dependence of nonlinear suppressive effects. These data raise the question of a modality-specific adaptational scaling of the spatial ranges of short- and long-range connections to the needs of interaction dimensions.

We are currently extending our approach to the analysis of moving stimuli and the role of stimulus history for the establishment of a moving trajectory of cortical activity. In addition, we initiated studies to explore the impact of plastic reorganizations on nonlinear interactions.

An ultimate goal would be to record neural activity simultaneously, which additionally allows insight into the ongoing dynamics of cooperative processes. Combining this technique with real-time optical imaging can provide insight into the cortical layout of the spatial interaction ranges and their implementation by anatomical connections.

Acknowledgements

This work was supported by the Deutsche Forschungsgemeinschaft and by the Institute for Neuroinformatics. D.J. holds a Minerva stipend. We thank our colleagues for extensive and extended discussions: Drs. Amir Akhavan, Wolfram Erlhagen, Martin Giese, Gregor Schöner, Axel Steinhage and Werner von Seelen. We also thank Luis Tissot for help in data analysis. We gratefully acknowledge the cooperation of Dr. Thomas Kalt in the studies of rat somatosensory cortex and for providing instructive material.

Appendix

Constructing two-dimensional distributions of population activity by Gaussian interpolation

For each location on the 6 × 6 grid, an average response strength was determined for each cell by averaging the firing rate in the time interval between 40 and 65 ms after stimulus onset corresponding to the peak responses in the PSTHs. RF profiles

were obtained and smoothed by convolution with a Gaussian profile in 2D (half width = 0.64°). The center of the RF of each cell was then computed as the center of mass of that part of the RF profile that exceeded half of the maximal firing rate.

The firing rate, $f_n(s, t)$ of neuron number n to stimulus number s was defined as the firing rate in a 10-ms time interval beginning at time t after stimulus onset, averaged over 32 stimulus repetitions. Spontaneous activity, b_n, was estimated as the mean firing rate accumulated over non-stimulus trials. For the purpose of constructing the population representation, the firing rate of each cell was normalized to its maximum firing rate, m_n, over all stimuli used to measure the response planes and during any single 10-ms bin in the time interval from stimulus onset to 100 ms after stimulus onset. This normalized firing rate

$$F_n(s, t) = \frac{f_n(s, t) - b_n}{m_n - b_n} \quad (1)$$

was always well defined and positive. The normalized firing rates, $F_n(s, t)$, were depicted at the position of each neuron's calculated RF center. For interpolation of the data points, the width of the Gaussian profile was chosen equal to 0.6° in the visual space (approximately corresponding to the average RF width of all neurons recorded (Fig. 2A)). To correct for uneven sampling of visual space by the limited number of RF centers, the distribution was normalized by dividing by a density function, which was simply the sum of unweighted Gaussian profiles (width = 0.64°) centered on all RF centers.

Calculation of population representations in the somatosensory cortex

To obtain population distributions that are defined for the parameter skin field location, the area of the hand-plotted RF was convoluted with a Gaussian, normalized to amplitude of unity. To be independent of this particular type of normalization, in a second approach, the same procedure was followed by normalizing the Gaussian distribution to integral of unity. To construct two-dimensional activity distributions across the skin the calculated Gaussians were summed. To correct for uneven sampling, the distribution was normalized by dividing by a density function, which was the sum of the unweighted Gaussian profiles. The resulting population representation reflects the local distribution of neuronal activation with highest amplitude at the actual location of a common stimulus encoded by the entire population.

References

Albus, K. (1975) A quantitative study of the projection area of the central and the paracentral visual field in area 17 of the cat. I. The precision of the topography. *Exp. Brain Res.*, 24: 159–179.

Allman, J., Miezin, F. and McGuiness, E.L. (1985) Stimulus specific responses from beyond the classical receptive field. *Annu. Rev. Neurosci.*, 8: 407–430.

Arieli, A., Sterkin, A., Grinvald, A. and Aertsen, A. (1996) Dynamics of ongoing activity: explanation of the large variability in evoked cortical responses. *Science*, 273: 1868–1871.

Barlow, H.B. (1972) Single units and sensation: a neuron doctrine for perceptual psychology? *Perception*, 1: 371–394.

Blasdel, G.G. and Salama, G. (1986) Voltage-sensitive dyes reveal a modular organization in monkey striate cortex. *Nature*, 321: 579–585.

Bonhoeffer, T. and Grinvald, A. (1991) Iso-orientation domains in cat visual cortex are arranged in pinwheel-like patterns. *Nature*, 353: 429–431.

Braitenberg, V. and Schüz, A. (1991) *Anatomy of the Cortex.* Springer, New York.

Braun, C., Schweizer, R., Elbert, T., Birbaumer, N. and Taub, E. (2000) Differential activation in somatosensory cortex for different discrimination tasks. *J. Neurosci.*, 20: 446–450.

Burkitt, G.R., Lee, J. and Ts'o, D.J. (1998) Functional organization of disparity in visual area V2 of the macaque monkey. *Soc. Neurosci. Abstr.*, 24: 1978.

Cauller, L.J., Clancy, B. and Connors, B.W. (1998) Backward cortical projections to primary somatosensory cortex in rats extend long horizontal axons in layer I. *J. Comp. Neurol.*, 390: 297–310.

Chapin, J.K. and Lin, C.S. (1984) Mapping the body representation in the SI cortex of anesthetized and awake rats. *Comp. Neurol.*, 229: 199–213.

Chapin, J.K., Moxon, K.A., Markowitz, R.S. and Nicolelis, M.A. (1999) Real-time control of a robot arm using simultaneously recorded neurons in the motor cortex. *Nat. Neurosci.*, 2: 664–670.

Das, A. and Gilbert, C.D. (1997) Distortions of visuotopic map match orientation singularities in primary visual cortex. *Nature*, 387: 594–598.

Das, A. and Gilbert, C.D. (1999) Topography of contextual modulations mediated by short-range interactions in primary visual cortex. *Nature*, 399: 655–661.

DiCarlo, J.J., Johnson, K.O. and Hsiao, S.S. (1998) Structure of receptive fields in area 3b of primary somatosensory cortex in the alert monkey. *J. Neurosci.*, 18: 2626–2645.

Diesmann, M., Gewaltig, M.O. and Aertsen, A. (1999) Stable propagation of synchronous spiking in cortical neural networks. *Nature*, 402: 529–533.

Dinse, H.R. (1986) Foreground–background-interaction — Stimulus dependent properties of the cat's area 17, 18 and 19 neurons outside the classical receptive field. *Perception*, 15: A6.

Dinse, H.R. and Jancke, D. (2001) Time-varient processing in V1: from microscopic (single cell) to mesoscopic (population) levels. *Trends Neurosci.*, 24: 203–205.

Dinse, H.R. and Schreiner, C.E. (2001) Do primary sensory areas play homologous roles in different sensory modalities? In: A. Schüz and R. Miller (Eds.), *Cortical Areas: Unity and Diversity: Conceptual Advances in Brain Research.* Harwood, in press.

Dinse, H.R., Jancke, D., Akhavan, A.C., Kalt, T. and Schöner, G. (1996) Dynamics of population representations of visual and somatosensory cortex based on spatio-temporal stimulation. In: S.I. Amari, L. Xu, L.W. Chan, I. King and K.S. Leung (Eds.), *Progress in Neural Information Processing. Interna-*

tional Conference on Neural Information Processing. ICONIP '96, Springer, Singapore, pp. 1285–1290.

Doetsch, G.S. (2000) Patterns in the brain. Neuronal population coding in the somatosensory system. *Physiol. Behav.*, 69: 187–201.

Erlhagen, W., Bastian, A., Jancke, D., Riehle, A. and Schöner, G. (1999) The distribution of neuronal population activation (DPA) as a tool to study interaction and integration in cortical representations. *J. Neurosci. Methods*, 94: 53–66.

Gallant, J.L., Connor, C.E. and van Essen, D.C. (1998) Neural activity in areas V1, V2 and V4 during free viewing of natural scenes compared to controlled viewing. *NeuroReport*, 9: 2153–2158.

Gardner, E.P. and Palmer, C. (1989) Simulation of motion on the skin. I. Receptive fields and temporal frequency coding by cutaneous mechanoreceptors of OPTACON pulses delivered to the hand. *J. Neurophysiol.*, 62: 1410–1436.

Gilbert, C.D. and Wiesel, T.N. (1985) Intrinsic connectivity and receptive field properties in visual cortex. *Vision Res.*, 25: 365–374.

Gilbert, C.D. and Wiesel, T.N. (1990) The influence of contextual stimuli on the orientation selectivity of cells in primary visual cortex of the cat. *Vision Res.*, 30: 1689–1701.

Gilbert, C., Ito, M., Kapadia, M. and Westheimer, G. (2000) Interactions between attention, context and learning in primary visual cortex. *Vision Res.*, 40: 1217–1226.

Hickmott, P.W. and Merzenich, M.M. (1998) Single-cell correlates of a representational boundary in rat somatosensory cortex. *J. Neurosci.*, 18: 4403–4416.

Hinton, G.E., McClelland, J.L. and Rumelhart, D.E. (1986) Distributed representations. In: J.A. Feldman, P.J. Hayes and D.E. Rumelhart (Eds.), *Parallel Distributed Processing. Exploration in the Microstructure of Cognition. Volume I: Foundations* MIT Press, Cambrige, MA, pp. 77–109.

Hock, H.S. and Eastman, K.E. (1995) Context effects on perceived position: sustained and transient temporal influences on spatial interactions. *Vision Res.*, 35: 635–646.

Hubel, D.H. and Wiesel, T.N. (1962) Receptive fields, binocular interaction and functional architecture in the cat's visual cortex. *J. Physiol.*, 160: 106–154.

Hubener, M., Shoham, D., Grinvald, A. and Bonhoeffer, T. (1997) Spatial relationships among three columnar systems in cat area 17. *J. Neurosci.*, 17: 9270–9284.

Jancke, D. (2000) Orientation formed by a spot's trajectory: A two-dimensional population approach in primary visual cortex. *J. Neurosci.* 20: RC86.

Jancke, D., Akhavan, A.C., Erlhagen, W., Giese, M., Steinhage, A., Schöner, G. and Dinse, H.R. (1996) Population coding in cat visual cortex reveals nonlinear interactions as predicted by a neural field model. In: C. von der Malsburg, W. von Seelen, J.C. Vorbrüggen and B. Sendhoff (Eds.), *Artificial Neural Networks — ICANN '96*, Springer, pp. 641–648.

Jancke, D., Erlhagen, W., Dinse, H.R., Akhavan, A.C., Giese, M., Steinhage, A. and Schöner, G. (1999) Parametric population representation of retinal location: neuronal interaction dynamics in cat primary visual cortex. *J. Neurosci.*, 19: 9016–9028.

Johnson, K.O. (1974) Reconstruction of population response to a vibratory stimulus in quickly adapting mechanoreceptive afferent fibre population innervating glabrous skin of the monkey. *J. Neurophysiol.*, 37: 48–72.

Kalt, T., Akhavan, A.C., Jancke, D. and Dinse, H.R. (1996) Dynamic population coding in rat somatosensory cortex. *Soc. Neurosci. Abstr.*, 22: 105.

Kanizsa, G. (1976) Subjective contours. *Sci. Am.*, 234: 48–52.

Kim, D.S., Matsuda, Y., Ohki, K., Ajima, A. and Tanaka, S. (1999) Geometrical and topological relationships between multiple functional maps in cat primary visual cortex. *NeuroReport*, 10: 2515–2522.

Kisvarday, Z.F., Toth, E., Rausch, M. and Eysel, U.T. (1997) Orientation-specific relationship between populations of excitatory and inhibitory lateral connections in the visual cortex of the cat. *Cereb. Cortex*, 7: 605–618.

Lehky, S.R. and Sejnowski, T.J. (1999) Seeing white: qualia in the context of decoding population codes. *Neural Comput.*, 11: 1261–1280.

LeVay, S., Stryker, M.P. and Shatz, C.J. (1978) Ocular dominance columns and their development in layer IV of the cat's visual cortex: a quantitative study. *J. Comp. Neurol.*, 179: 223–244.

Löwel, S. and Singer, W. (1992) Selection of intrinsic horizontal connections in the visual cortex by correlated neuronal activity. *Science*, 255: 209–212.

Mendola, J.D., Dale, A.M., Fischl, B., Liu, A.K. and Tootell, B.H. (1999) The representation of illusory and real contours in human cortical visual areas revealed by functional magnetic resonance imaging. *J. Neurosci.*, 19: 8560–8572.

Merzenich, M.M., Nelson, R.J., Stryker, M.P., Cynader, M.S., Schoppmann, A. and Zook, J.M. (1984) Somatosensory cortical map changes following digit amputation in adult monkeys. *J. Comp. Neurol.*, 224: 591–605.

Müsseler, J., Van der Heijden, A.H.C., Mahmud, S.H., Deubel, H. and Ertsey, S. (1999) Relative mislocalization of briefly presented stimuli in the retinal periphery. *Percept. Psychophys.*, 61: 1646–1661.

Nicolelis, M.A.L. (1996) Beyond maps: a dynamic view of the somatosensory system. *Braz. J. Med. Biol. Res.*, 29: 401–412.

Nicolelis, M.A.L. (Ed.) (1999) *Methods in Neural Ensemble Recordings*. CRC Press, New York.

Nicolelis, M.A., Ghazanfar, A.A., Stambaugh, C.R., Oliveira, L.M., Laubach, M., Chapin, J.K., Nelson, R.J. and Kaas, J.H. (1998) Simultaneous encoding of tactile information by three primate cortical areas. *Nat. Neurosci.*, 1: 621–630.

Ramachandran, V.S., Ruskin, D., Cobb, S. and Rogers-Ramachandran, D. (1994) On the perception of illusory contours. *Vision Res.*, 34: 3145–3152.

Salinas, E. and Abbott, L.F. (1994) Vector reconstruction from firing rates. *J. Comp. Neurosci.*, 1: 89–107.

Schreiner, C.E. (1995) Order and disorder in auditory cortical maps. *Curr. Opin. Neurobiol.*, 5: 489–496.

Segev, I. and Rall, W. (1998) Excitable dendrites and spines: earlier theoretical insights elucidate recent direct observations. *Trends Neurosci.*, 21: 453–460.

Sheth, B.R., Sharma, J., Rao, S.C. and Sur, M. (1996) Orien-

tation maps of subjective contours in visual cortex. *Science*, 274: 2110–2115.

Shoham, D., Hubener, M., Schulze, S., Grinvald, A. and Bonhoeffer, T. (1997) Spatio-temporal frequency domains and their relation to cytochrome oxidase staining in cat visual cortex. *Nature*, 385: 529–533.

Sillito, A.M., Grieve, K.L., Jones, H.E., Cudeiro, J. and Davis, J. (1995) Visual cortical mechanisms detecting focal orientation discontinuities. *Nature*, 378: 492–496.

Sterr, A., Muller, M.M., Elbert, T., Rockstroh, B., Pantev, C. and Taub, E. (1998) Perceptual correlates of changes in cortical representation of fingers in blind multifinger Braille readers. *J. Neurosci.*, 18: 4417–4423.

Sur, M., Angelucci, A. and Sharma, J. (1999) Rewiring cortex: the role of patterned activity in development and plasticity of neocortical circuits. *J. Neurobiol.*, 41: 33–43.

Swindale, N.V. (2000) How many maps are there in visual cortex? *Cereb. Cortex*, 10: 633–643.

Swindale, N.V., Matsubara, J.A. and Cynader, M.S. (1987) Surface organization of orientation and direction selectivity in cat area 18. *J. Neurosci.*, 7: 1414–1427.

Szulborski, R.G. and Palmer, L.A. (1990) The two-dimensional spatial structure of nonlinear subunits in the RFs of complex cells. *Vision Res.*, 30: 249–254.

Thier, P., Dicke, P.W., Haas, R. and Barash, S. (2000) Encoding of movement time by populations of cerebellar Purkinje cells. *Nature*, 405: 72–76.

Tsodyks, M., Kenet, T., Grinvald, A. and Arieli, A. (1999) Linking spontaneous activity of single cortical neurons and the underlying functional architecture. *Science*, 286: 1943–1946.

Tusa, R.J., Palmer, L.A. and Rosenquist, A.C. (1978) The retinotopic organization of area 17 (striate cortex) in the cat. *J. Comp. Neurol.*, 177: 213–235.

Von der Heydt, R., Peterhans, E. and Baumgartner, G. (1984) Illusory contours and cortical neuron responses. *Science*, 224: 1260–1262.

Weliky, M., Bosking, W.H. and Fitzpatrick, D. (1996) A systematic map of direction preference in primary visual cortex. *Nature*, 379: 725–728.

Westheimer, G. (1979) Cooperative neural processes involved in stereoscopic acuity. *Exp. Brain Res.*, 36: 585–597.

Westheimer, G. (1990) Simultaneous orientation contrast for lines in the human fovea. *Vision Res.*, 30: 1913–1921.

Wiesel, T.N., Hubel, D.H. and Lam, D.M. (1974) Autoradiographic demonstration of ocular-dominance columns in the monkey striate cortex by means of transneuronal transport. *Brain Res.*, 79: 273–279.

Young, T. (1802) II. The Bakerian Lecture. On the theory of light and colors. *Phil. Trans. R. Soc. Lond.* 91: 12–48.

Zhang, K. and Sejnowski, T.J. (1999) A theory of geometric constraints on neural activity for natural three-dimensional movement. *J. Neurosci.*, 19: 3122–3145.